

## PAL LINAC UPGRADE FOR A 1-3 Å XFEL

J. S. Oh, W. Namkung, Pohang Accelerator Laboratory, POSTECH, Pohang 790-784, Korea  
Y. Kim, Deutsches Elektronen-Synchrotron DESY, D-22603 Hamburg, Germany

### Abstract

With the successful SASE FEL saturation at 80-nm wavelength at TTF1, TTF2 will begin re-commissioning in the fall of 2004 as an FEL user facility to 6 nm with 1-GeV beams. The high gain harmonic generation is also confirmed by the DUV-FEL experiments at 266 nm with seeding wavelength at 800 nm. In order to realize a hard X-ray SASE FEL (SASE XFEL) with a lower energy beams, we need a long in-vacuum mini-gap undulator and a GeV-scale FEL driving linac that can supply an extremely low slice emittance, a high peak current, and an extremely low slice energy spread. PAL is operating a 2.5-GeV electron linac as a full-energy injector to the PLS storage ring. By adding an RF photo-cathode gun, two bunch compressors, and a 0.5-GeV S-band injector linac to the existing PLS linac, and by installing a 60-m long in-vacuum undulator, the PLS linac can be converted to a SASE XFEL facility (PAL XFEL) which supplies coherent X-ray down to 0.3-nm wavelength. The third harmonic enhancement technique can supply coherent hard X-ray beams to 0.1 nm. The technical parameters related to these goals are examined, and preliminary design details are reviewed for the PAL linac upgrade idea for a 1-3 Å PAL XFEL.

### INTRODUCTION

The requirements of X-ray from scientific users are radiation wavelength of 0.1nm, pulse length of 20 fs (FWHM). PAL operates a 2.5-GeV electron linac, the 3<sup>rd</sup> largest in the world, as a full-energy injector to the PLS storage ring [1]. The PAL 2.5-GeV linac can be converted to an X-ray free electron laser (XFEL) facility driven by a self-amplified spontaneous emission (SASE) mode, which supplies coherent X-rays down to 0.3-nm wavelength. The third harmonic enhancement technique on the electron beam or advanced X-ray laser optics will be applied to obtain radiation wavelengths of 0.1 nm. The design goal is for the undulator to be less than 60 m in total length. The linac should supply highly bright 3-GeV beams to a 60-m long in-vacuum undulator with a 3-mm gap and a 12.5-mm period, of which emittance of 1.5 mm-mrad, a peak current of 4 kA, and a low energy spread of 0.02% [2].

Table 1 shows the comparison of single bunch specifications between the PLS linac and PAL XFEL. Normalized emittance should be 100 times improved, which requires a low emittance gun and high gradient acceleration at low energy region to preserve the emittance. The suitable bunch compression is one of key technique to realize the high peak current, also.

Questions are how to utilize the existing 2.5-GeV linac and how to keep the operation mode as a full energy injector for PLS 2.5-GeV storage ring.

Therefore we have to minimize the modification of existing linac layout. We have to find matching conditions to provide flexible beam operation for both applications. Also the site is already fixed and limits the maximum size of a new machine scale. The performance and stability of the 2.5-GeV linac is also challenging to meet the strict SASE requirements.

Table 1: Bunch specifications of PLS linac and XFEL

Parameter	PLS Linac	XFEL
Beam energy	2.5 GeV	3.0 GeV
Normalized emittance	150 $\mu\text{m-rad}$	1.5 $\mu\text{m-rad}$
FWHM bunch length	13 ps	0.23 ps
RMS energy spread	0.26%	0.02%
Bunch charge	0.43 nC*	1.0 nC
Peak current	33 A*	4 kA
Repetition rate	10 Hz	60 Hz

\* 2-A gun current and 62% transmission

### PAL XFEL PROGRAM

The fundamental radiation wavelength  $\lambda_x$  of an undulator is given by

$$\lambda_x = \frac{\lambda_u}{2\gamma^2} (1 + K^2 / 2), \quad \gamma = E_o / 0.511, \quad K = 0.934 B_u \lambda_u,$$

where  $E_o$  is the beam energy in MeV,  $B_u$  is the peak magnetic field of the undulator in Tesla, and  $\lambda_u$  is the undulator period in cm. The peak magnetic field  $B_u$  of a 45°-magnetized undulator with  $H = \lambda_u/2$  is given by

$$B_u = \frac{4\sqrt{2}B_r}{\pi} \sum_{n=1,5,9}^{\infty} \frac{1}{n} (1 - e^{-2n\pi H/\lambda_u}) e^{-n\pi g/\lambda_u},$$

where  $B_r$  is assumed 1.19 Tesla with Nd<sub>2</sub>Fe<sub>14</sub>B magnets,  $H$  is the block height, and  $g$  is full-gap length [3]. Fig. 1 shows the undulator geometry with 45°-magnetization.

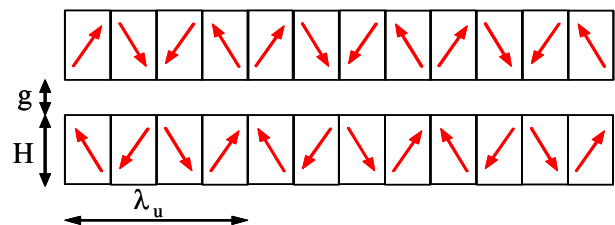


Figure 1: Undulator geometry with 45°-magnetization.

Either a short-period undulator or a high-energy beam can provide short-wave radiation. A short-period undulator will give a compact FEL machine for a short-wave radiation. It is important to keep reasonably large undulator parameter K to obtain a short saturation length. An in-vacuum mini-gap undulator can meet this idea that was introduced by the SCSS project at SPring-8 [4]. Fig. 2 shows the 0.3-nm XFEL curves with saturation lengths of 40, 50, 60 m and beam energy of 2.5, 3.0, 3.5 GeV, respectively. The one of possible solution that is reasonably economic, to meet the saturation length less than 60 m with margin is to use 3-GeV beam with a 3-mm gap and a 12.5-mm period for a undulator.

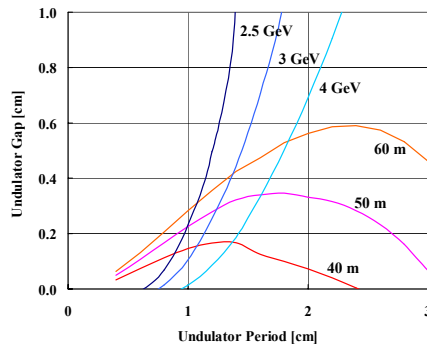


Figure 2: Undulator period and gap length for 0.3-nm SASE for saturation lengths (40, 50, 60 m) and beam energy (2.5, 3, 4 GeV).

Table 2 summarizes the FEL parameters for a 0.3-nm PAL-XFEL. The undulator beta value is adjusted to obtain as short a saturation length as possible. Undulator saturation length is approximately 20 times 3D gain length  $L_g$ .

Table 2: FEL parameters for 0.3-nm PAL XFEL

Undulator period [mm]	12.5
Undulator gap [mm]	3.0
Peak magnetic field [T]	0.97
Undulator parameter, K	1.14
Beta [m]	15
Saturation length [m]	52
FEL parameter	4.3e-4
1D gain length [m], $L_{1d}$	1.35
3D gain length correction, $\eta^*$	0.97
Gain length [m], $L_g$	2.67
Peak power [GW]	2.1
Peak brightness [ $\times 10^{32}$ ]**	1.4

\*  $L_g = (1+\eta) L_{1d}$   
 \*\* photons/sec-mm<sup>2</sup>-mrad<sup>2</sup>-0.1%BW

The 3D gain length correction and 3D gain length according to normalized emittance are calculated according to M. Xie [5] and shown in Fig. 3. In general, the electron beam emittance is required to be equal or less than the natural emittance of the FEL radiation. The gain correction factor of PAL XFEL is a bit larger than the LCLS and TESLA XFEL due to rather large normalized

emittance relative to the natural radiation emittance. However, due to the small periodic length of an undulator, the gain length becomes small. Therefore, it is possible to realized compact X-ray FEL by an in-vacuum undulator with small period and rather a low energy linear accelerator.

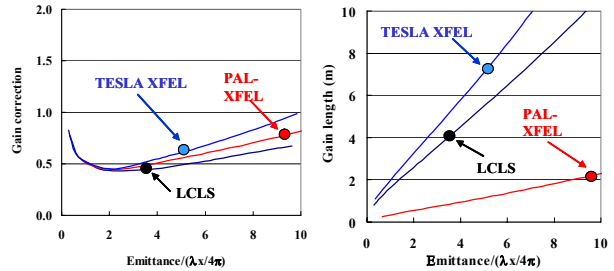


Figure 3: 3D Gain length and 3D gain correction factor.

The solid line ‘PAL XFEL’ in Fig. 4 shows the expected peak brilliance of the fundamental radiation of PAL-XFEL. The three circles on the line correspond to beam energies of 2.0, 2.5, and 3.0 GeV. The peak brilliance of PAL-XFEL is  $10^{12}$  time higher than the U7 undulator radiation from the PLS 3<sup>rd</sup> generation storage ring. The spontaneous radiation from the undulator of PAL XFEL is also a hard X-ray and  $10^{10}$  times brighter than the synchrotron radiation from the PLS bending magnet.

The ‘PAL VUV FEL’ assumes to use a conventional undulator with a period of 3 cm and a gap length of 1.2 cm to generate 1-4 nm VUV radiation by changing the beam energy from 1.5-3.0 GeV. The ‘PAL 0.1-nm XFEL’ denotes the possible 0.1-nm PAL-XFEL with the third harmonic enhancement technique employing an additional undulator with a shorter periodic length.

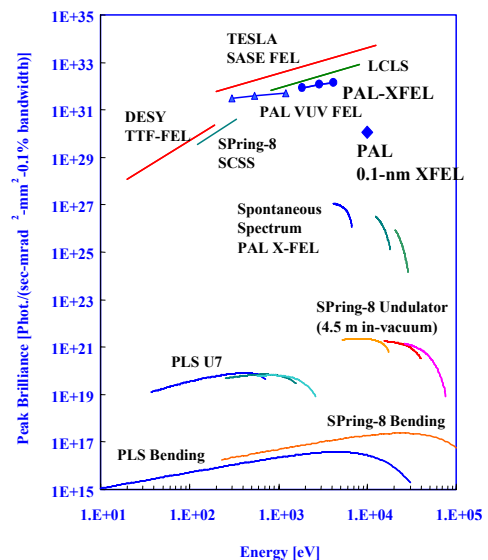


Figure 4: Peak brilliance for PAL XFEL.

### PLS LINAC UPGRADE

The existing 2.5-GeV S-band PLS linac can be converted to X-ray FEL driver with a new S-band photo-injector, and a new S-band FEL injector linac, two bunch compressors. Fig. 5 shows one of possible upgrade layout of the PAL linac including a new undulator system (U1 to U13). The injector consists of a low-emittance laser-driven photo-cathode gun, three S-band accelerating modules (X1, X2, X3), and two bunch compressors (BC1, BC2).

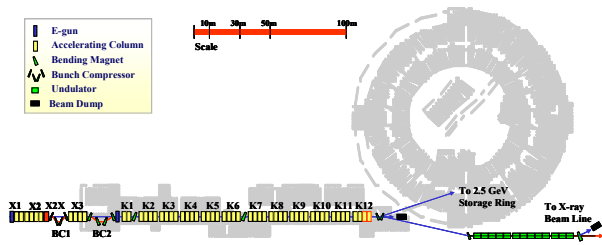


Figure 5: PLS linac upgrade scheme for PAL XFEL.

The previous design concept of an injector system presented in FEL2003 is somewhat improved in this work [2]. First of all, the dog-leg scheme in the new injector is modified to align the center line of the new injector to the one of existing linac to suppress emittance degradation due to CSR as possible as. Also two bunch compressors are located in the new injector system to minimize the modification of existing layout of PLS 2.5-GeV linac.

The S-band photo-injector is consisted of a Cu cathode and 1.6-cell S-band RF cavity. Table 3 shows beam parameters at the cathode. The photoelectron beam is generated by 10-ps, 500-μJ, and 260-nm UV laser. It is accelerated to 7 MeV by a high gradient of 120 MV/m within 16.8-cm length. The high gradient acceleration is essential to preserve the beam emittance under high space charge force at the low energy.

Table 3: Beam parameters at the cathode

Bunch length	10 ps (FWHM), 2.9 ps (rms)
Rise time (10-90%)	0.7 ps
Spot size	0.6 mm (rms)
Thermal emittance	0.6 μm
Peak gradient	120 MV/m
Peak solenoid field	2.71 kG at 19.1 cm

The lattice design is shown in Fig. 6 from the new injector to the end of main linac. The existing quadrupole magnets along the main linac are optimised as it is. Twiss parameters in the existing linac are possible to be re-optimised. Lattice optimisation is to find solution to minimize the second term in the following equation for the relative emittance growth [6]. The optimum condition is given when the alpha value is about 0 and beta function is about 3.

$$\frac{\varepsilon}{\varepsilon_0} = \sqrt{1 + \frac{(0.22)^2 \gamma_e^2 N^2}{36 \gamma \varepsilon_N \beta} \left( \frac{|\theta|^5 L_B}{\sigma_z^4} \right)^2 \frac{2}{3} [L_B^2 (1 + \alpha^2) + 9\beta^2 + 6\alpha\beta L_B]}$$

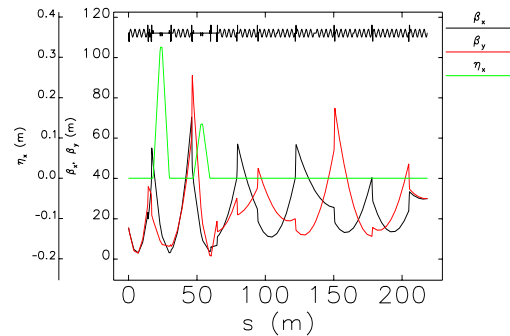


Figure 6: Lattice profile along the linac.

Against projected parameter dilution due to CSR and chromatic effect, adopted lattice design concepts are as follows: long drift space to reduce bending angle for a required momentum compaction R56, small bending angle at a large energy spread, large compression factor at BC1 and small compression factor at BC2. Strong focusing lattice around BC to reduce CSR induced emittance growth, small quadrupole length around BCs to reduce the chromatic effects, smaller maximum beta-function of ~ 60 m at BC1 entrance, larger maximum beta-function at BC2 entrance after reducing energy spread at BC2 are also effective. Against slice parameter dilution due to the micro-bunching instability, following design concepts are adopted: normal 4-bend chicane instead of S-type chicane, large uncorrelated energy spread at BC2 by putting the BC2 at low energy region. We do not consider laser beam heater or super conducting wiggler. Against the tight jitter tolerance, followings are considered: two stage BC, RF gun driven by its own klystron, each S-band accelerating column before BC2 driven by each own klystron, X-band correction cavity possibly driven by two X-band klystrons. Fig. 7 shows the detail layout of a new FEL injector linac including two bunch compressors and new accelerators. X2 is a modulator to make suitable energy spread for bunch compression. X2X is a linearizer of non-linear energy spread caused in the modulator.

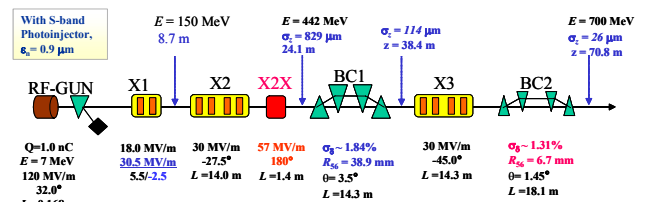


Figure 7: BCs and a new accelerator layout.

Detail layout of BC1 is shown in Fig. 8. The net chicane length is 12.2 m. Maximum beam offset from the centerline is 33 cm. The total chicane length becomes 17 m including focusing quadrupoles.

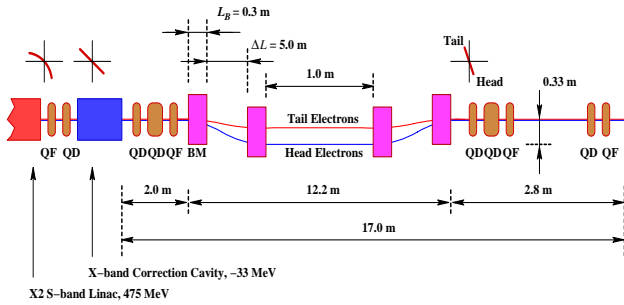


Figure 8: Detail layout of BC1.

Table 4 shows the design parameters of bunch compressor BC1 and BC2. BC2 layout is almost same as BC1. All uncorrelated energy spread is estimated at  $\pm 0.1$  mm core region. Initial uncorrelated energy spread at BC2 is increased after compression by BC1. The uncorrelated energy deviation at BC2 is larger than  $1 \times 10^{-5}$  that is required to suppress the micro-bunching instability.

Table 4: Design parameters of bunch compressors

Parameter	BC1	BC2
BC type	Two stage	Two stage
Beam energy	442 MeV	700 MeV
Relative energy spread	1.84%	1.31%
Uncorrelated energy spread	$9.2 \times 10^{-6}$	$4.3 \times 10^{-5}$
Bending angle	3.50 deg	1.45 deg
Momentum compaction R56	38.9 mm	6.70 mm
Total chicane length	12.2 m	12.2 m
Dipole length	0.3 m	0.3 m
Drift length $\Delta L$	5.0 m	5.0 m
Initial rms bunch length	820 $\mu\text{m}$	114 $\mu\text{m}$
Final rms bunch length	114 $\mu\text{m}$	26 $\mu\text{m}$
Compression factor	7.2	4.38
Initial projected emittance	0.90 $\mu\text{m}$	1.01 $\mu\text{m}$
Final projected emittance	1.01 $\mu\text{m}$	1.12 $\mu\text{m}$

### S2E SIMULATION

We examined beam parameters by the ASTRA simulation considering the space charge force at low energy. Lattice is designed by using ELEGANT code from X2 accelerating unit to the end of existing linac, which includes CSR effect in the bunch compressor and geometric wake field effect in the accelerating columns. The number of simulated particles is 200,000 in this study.

The energy spread along the bunch length is linearized by X-band linac as shown in Fig. 9. At the entrance of BC1, beam energy is 441.5 MeV, energy spread is 1.835%, beam size is 230  $\mu\text{m}$  ( $\sigma_x$ ), and 147  $\mu\text{m}$  ( $\sigma_y$ ), bunch length is 829  $\mu\text{m}$ , emittance is 0.953  $\mu\text{m}$  ( $\epsilon_{nx}$ ) and 0.945  $\mu\text{m}$  ( $\epsilon_{ny}$ ).

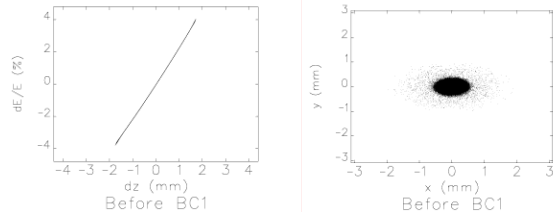


Figure 9: Phase spaces before BC1.

At the end of linac, beam energy is 3.389 GeV, energy spread is 0.033%, beam size is 68.1  $\mu\text{m}$  ( $\sigma_x$ ), and 61.9  $\mu\text{m}$  ( $\sigma_y$ ), bunch length is 26  $\mu\text{m}$ , normalized emittance is 1.116  $\mu\text{m}$  ( $\epsilon_{nx}$ ) and 1.004  $\mu\text{m}$  ( $\epsilon_{ny}$ ) in this simulation. Longitudinal short-range wake-field damps the energy spread at the tail region so that the energy profile along the bunch becomes more flat and uniform as shown in Fig. 10.

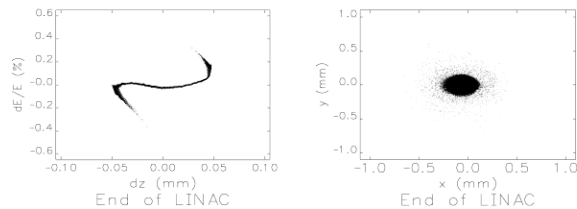


Figure 10: Phase spaces at the end of linac.

Fig. 11 shows the variation of the energy spread and the bunch length along the linac. The relative energy spread is continuously increased to 1.84% until the entrance of BC1 to fit the necessary compression factor. The variation of energy spread in the BC2 is kept low by small CSR effect. Increasing the beam energy, the energy spread is continuously decreased to 0.03% at the end of linac. The large compression at BC1 and small compression at BC2 are clearly shown in the figure.

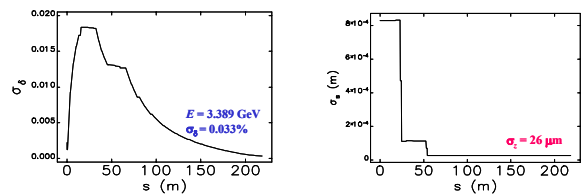


Figure 11: Energy spread and bunch length along linac.

Fig. 12 shows the beam quality at the end of linac. The required beam parameters for FEL lasing at the undulator entrance correspond to dotted lines for the peak current of 4 kA, normalized emittance of 1.5  $\mu\text{m}$ , and energy spread of 0.02%. The normalized emittance, that is most sensitive FEL parameter, is well below the requirement along the whole bunch, which gives reasonable margin for safe saturation within 60-m long undulator. The lowest peak current along the bunch is about 20% less than 4 kA. The slice emittance is also 20% lower than the nominal value of 1.5  $\mu\text{m}$ . Because the saturation length is

more sensitive to the emittance, it is safe to make saturation along the whole bunch.

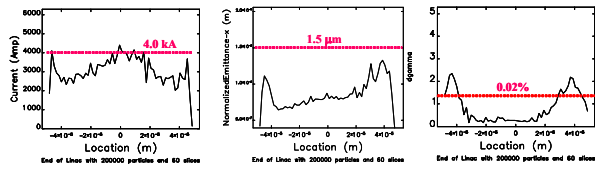


Figure 12: Beam quality at the end of linac.

**DISCUSSION**

Fig. 13 shows the sensitivity of saturation length on the system performance for beam emittance, energy spread, bunch length, and undulator beta value. The system parameters are normalized by the nominal values. The most sensitive parameter is the emittance of the electron beam. Therefore a low emittance gun is essential for PAL XFEL.

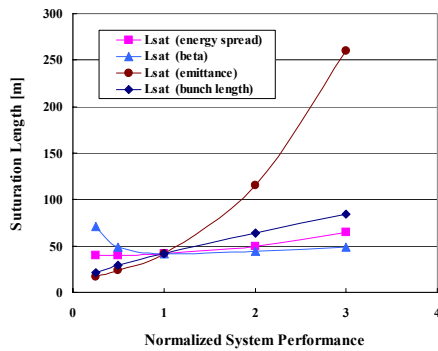


Figure 13: Saturation length vs. system performance.

Fig. 14 shows the distribution of uncorrelated energy spread along the bunch length. At the entrance of BC1, uncorrelated energy deviation at ± 1.0 mm core is 4 keV at the beam energy of 442 MeV. It is increase to 30 keV by high compression factor at the BC1. If we consider space charge force, this will be increased further at BC2. The increased uncorrelated energy spread at the BC2 suppresses micro-bunching instabilities.

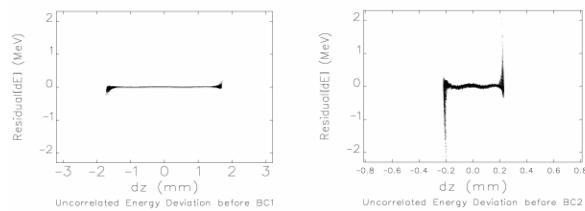


Figure 14: Uncorrelated energy spread at the entrance of BC1 and BC2.

The bunch length can be made shorter by the slit placed in the middle of bunch compressor [7]. The bunch length at the center of BC2 is 70 μm and the transverse beam size is 1.74 mm as shown in Fig. 15. The shaded area represents a 300-μm slit at this location. By adding the slit, the head and tail parts of the bunch can be removed. Then the bunch length can be further reduced down to 20 fs.

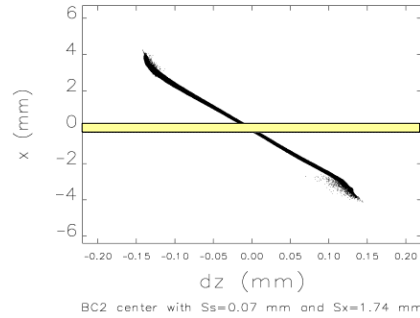


Figure 15: Beam size at the center of BC2.

The wake field effect on the electron beams in the undulator and the beam quality degradation due to the magnet field error are sensitive to FEL process. The jitter and sensitivity analysis on the combined parameter space is to be intensively followed. It is necessary to analyse hardware upgrade scheme and stability requirements with related technical parameters.

**ACKNOWLEDGMENTS**

This work is supported by POSCO and the Ministry of Science and Technology (MOST) of Korea.

**REFERENCES**

- [1] <http://pal.postech.ac.kr/>
- [2] J. S. Oh et al., "0.3-nm SASE FEL at PAL," Nucl. Instr. Meth. A528, 582 (2004)
- [3] Maréchal X., Chavanne J., Elleaume P., On 2D periodic magnetic field, ESRF-SR/ID 90-38 (1990)
- [4] T. Shintake et al., "SPring-8 Compact SASE Source (SCSS)," in Proc. the SPIE2001, San Diego, USA, 2001; <http://www-xfel.spring8.or.jp>
- [5] M. Xie, "Design Optimization for an X-ray Free Electron Laser Driven by SLAC Linac," LBL Preprint No-36038, 1995
- [6] T. Limberg, "Emittance Growth in the LCLS due to Coherent Synchrotron Radiation," SLAC internal note, Oct. 1997
- [7] P. Emma et al. SLAC-PUB-10002